online data

Clinical Science (2012) **122**, 409–419 (Printed in Great Britain) doi:10.1042/CS20110257 409

Dissociation of ERK signalling inhibition from the anti-amyloidogenic action of synthetic ceramide analogues

Hongyun LI*†, Genevieve EVIN‡§, Andrew F. HILL§‖, Ya Hui HUNG§¶, Ashley I. BUSH§ and Brett GARNER*†

*Illawarra Health and Medical Research Institute, University of Wollongong, Wollongong, NSW 2522, Australia, †School of Biological Sciences, University of Wollongong, Wollongong, NSW 2522, Australia, ‡Department of Pathology, University of Melbourne, Melbourne, VIC 3010, Australia, §Mental Health Research Institute, University of Melbourne, Melbourne, VIC 3010, Australia, ||Department of Biochemistry and Molecular Biology, Bio21 Institute, University of Melbourne, Melbourne, VIC 3010, Australia, and ¶Centre for Neuroscience, University of Melbourne, Melbourne, VIC 3010, Australia

ABSTRACT

Inhibition of GSL (glycosphingolipid) synthesis reduces Aβ (amyloid β-peptide) production *in vitro*. Previous studies indicate that GCS (glucosylceramide synthase) inhibitors modulate phosphorylation of ERK1/2 (extracellular-signal-regulated kinase 1/2) and that the ERK pathway may regulate some aspects of Aβ production. It is not clear whether there is a causative relationship linking GSL synthesis inhibition, ERK phosphorylation and Aβ production. In the present study, we treated CHO cells (Chinese-hamster ovary cells) and SH-SY5Y neuroblastoma cells, that both constitutively express human wild-type APP (amyloid precursor protein) and process this to produce Aβ, with GSL-modulating agents to explore this relationship. We found that three related ceramide analogue GSL inhibitors, based on the PDMP (D-*threo*-1-phenyl-2-decanoylamino-3-morpholino-1-propanol) structure, reduced cellular Aβ production and in all cases this was correlated with inhibition of pERK (phosphorylated ERK) formation. Importantly, the L-*threo* enantiomers of these compounds (that are inferior GSL synthesis inhibitors compared with the D-*threo*-enantiomers) also reduced ERK phosphorylation to a similar extent without altering Aβ production. Inhibition of ERK activation using either PD98059 [2-(2-amino-3-methoxyphenyl)-4H-1-benzopyran-4-one] or U0126 (1,4-diamino-2,3-dicyano-1,4-bis[2-aminophenylthio] butadiene) had no impact on Aβ production, and knockdown of endogenous GCS using small interfering RNA reduced cellular GSL levels without suppressing Aβ production or pERK formation. Our data suggest that the alteration in pERK levels following treatment with these ceramide analogues is not the principal mechanism involved in the inhibition of Aβ generation and that the ERK signalling pathway does not play a crucial role in processing APP through the amyloidogenic pathway.

Key words: Alzheimer's disease, amyloid β-peptide, amyloid precursor protein, extracellular-signal-regulated kinase (ERK), glycosphingolipid.

Abbreviations: 2AA, 2-anthranilic acid; Aβ, amyloid β-peptide; Aβ40, Aβ-(1–40); Aβ42, Aβ-(1–42); AD, Alzheimer's disease; APP, amyloid precursor protein; BACE-1, β-site APP-cleaving enzyme; CHO cell, Chinese-hamster ovary cell; DAPT, *N*-[*N*-(3,5-difluorophenacetyl)-L-alanyl]-(*S*)-phenylglycine t-butyl ester; ERK, extracellular-signal-regulated kinase; EtDO-P4, D-*threo*-ethylenedioxy-1-phenyl-2-palmitoylamino-3-pyrrolidino-1-propanol; FBS, fetal bovine serum; GAPDH, glyceraldehyde-3-phosphate dehydrogenase; GCS, glucosylceramide synthase; GlcCer, glucosylceramide; GSL, glycosphingolipid; LacCer, lactosylceramide; MAPK, mitogen-activated protein kinase; MTT, 3-(4,5-dimethylthiazol-2-yl)-2,5-2*H*-tetrazolium bromide; PDMP, D-*threo*-1-phenyl-2-decanoylamino-3-morpholino-1-propanol; pERK, phosphorylated ERK; PPMP, D-*threo*-1-phenyl-2-hexadecanoylamino-3-morpholino-1-propanol; PS, presenilin; sAPPα, soluble APPα fragment; siRNA, small interfering RNA.

Correspondence: Professor Brett Garner (email brettg@uow.edu.au).

INTRODUCTION

Amyloid plaques are a key pathological feature of AD (Alzheimer's disease) [1], a common neurodegenerative disorder affecting our aging population. Amyloid plaques are enriched with Aβ (amyloid β-peptide) peptides that are derived from the proteolytic processing of the APP (amyloid precursor protein) [2]. APP can be proteolytically processed by the α-secretase pathway that does not generate Aβ as the metalloproteases [such as ADAM-10 (a disintegrin and metalloproteinase 10)] responsible cleave in the middle of the Aβ sequence. In an alternative pathway, sequential cleavage of APP by β-secretase [BACE-1 (β-site APP-cleaving enzyme)] and γ-secretase [a complex containing PS-1 (presenilin 1) or PS-2 as the catalytic subunit] generates neurotoxic Aβ peptides predominantly of 40 or 42 amino acids [3–6]. In addition to factors that regulate the rate of Aβ production, the ratio of Aβ40 [Aβ-(1–40)] to Aβ42 [Aβ-(1–42)] species generated, their propensity to form macromolecular complexes and their catabolism and clearance from the central nervous system are all relevant therapeutic targets for AD [3,7]. Despite the recognized role for Aβ in AD neurodegeneration, the factors that modify Aβ production and deposition are not completely understood.

Previous studies have suggested that specific GSLs (glycosphingolipids) may promote Aβ production and/or its assembly into neurotoxic complexes [8–13]. GSLs co-localize with Aβ in amyloid plaques and it has been proposed that ganglioside G_{M1} interacts with Aβ to form a seed for amyloid plaque formation [14]. Other studies have shown that G_{M1} can act on mature Aβ fibrils in amyloid plaque to regenerate neurotoxic Aβ protofibrils [15]. In addition, when GD3 synthase-knockout mice (phenotype characterized by reductions in the levels of several brain gangliosides) were crossed with APPswe + PSEN1DE9 amyloidogenic mice (a mouse model of AD displaying both amyloid plaque pathology and cognitive impairments), both soluble Aβ and plaque load were reduced (85–95 %) and this was associated with improved cognitive performance [16]. These data imply that pharmacological inhibition of GSL synthesis may be beneficial in the AD/amyloidogenesis context.

A previous study has shown that the GSL synthesis inhibitor PDMP (D-1-phenyl-2-decanoylamino-3-morpholino-1-propanol) reduced Aβ secretion from SH-SY5Y neuroblastoma cells by ~55 % when used at a concentration of 25 μM for a 48 h period [10]. In recent studies, we have shown that two more potent GSL synthesis inhibitors, PPMP (D-*threo*-1-phenyl-2-hexadecanoylamino-3-morpholino-1-propanol) and EtDO-P4 (D-*threo*-ethylenedioxy-1-phenyl-2-palmitoylamino-3-pyrrolidino-1-propanol), inhibit Aβ secretion both from CHO cells (Chinese-hamster ovary cells) stably expressing human APP695 (CHO-APP) and from primary human neurons with IC_{50} values in the low (1–5) micromolar range [17]. Although the D-*threo*-enantiomers of these ceramide analogues have been shown to have a high degree of specificity for GCS (glucosylceramide synthase) [18–23], downstream effects on membrane lipid microdomain structure, cellular ceramide metabolism and signalling pathways may also be involved. For example, modulation of membrane GSL levels by PDMP and related compounds has an impact on membrane cholesterol transport and EGFR (epidermal growth factor receptor) signalling [24,25]. PDMP has also been shown to inhibit ERK (extracellular-signal-regulated kinase) phosphorylation in neural precursor cells [26] and this is potentially important in the current context as there is evidence that the ERK pathway is dysregulated in AD [27–29] and that ERK activation may regulate APP proteolysis and/or Aβ production *in vitro* [30–32].

In the present study, we have investigated the enantiomer-specific actions of PPMP and EtDO-P4 on both cellular Aβ production and ERK signalling. We also directly assess the impact that ERK inhibitors and siRNA (small interfering RNA)-mediated silencing of GCS has on cellular Aβ production.

MATERIALS AND METHODS

Materials

Synthetic ceramide analogues PDMP, D-PPMP and L-PPMP were purchased from Matreya. D/L-EtDO-P4 was synthesized as described previously [20]. The D- and L-EtDO-P4 enantiomers were purified by preparative normal phase HPLC using a Lux 5 μm Cellulose-2 AXIA packed chiral 250 mm × 21.2 mm column (Phenomenexa). An Agilent 1100 HPLC system was used with a mobile phase hexane/propan-2-ol/diethylamine (85:15:0.1, by vol.), a flow rate of 10 ml/min and UV detection at 220 nm. D-EtDO-P4 eluted at 25 min and was collected from the column and dried under vacuum before use in experiments. The γ-secretase inhibitor DAPT (*N*-[*N*-(3,5-difluorophenacetyl)-L-alanyl]-(*S*)-phenylglycine t-butyl ester) and the MAPK (mitogen-activated protein kinase) pathway inhibitors PD98059 (2-(2-amino-3-methoxyphenyl)-4H-1-benzopyran-4-one) and U0126 (1,4-diamino-2,3-dicyano-1,4-bis[2-aminophenylthio] butadiene) were purchased from Sigma. Purified leech (*Macrobdella decora*) ceramide glycanase (EC 3.2.1.123) was from V-Labs. Cell culture medium and additives were obtained from Invitrogen unless stated otherwise. All organic solvents were of analytical grade and were purchased from Ajax Finechem. All other reagents were purchased through standard commercial suppliers.

Cell culture

The CHO cell line stably expressing the human 695-amino-acid isoform of APP (CHO-APP) was generated

and maintained as described previously [33,34]. CHO-APP cells were cultured in RPMI 1640 medium containing 10 % (v/v) FBS (fetal bovine serum), 2 mM glutamine, 100 units/ml penicillin and 100 μg/ml streptomycin. The cells were cultured in the presence of puromycin (7.5 μg/ml) to maintain selection for the expression plasmid. The SH-SY5Y-APP cell line was generated by transfecting human SH-SY5Y neuroblastoma cells with cDNA containing wild-type human APP695 cloned into the pIRESpuro2 vector [35]. Stably transfected cells were selected using 2 μg/ml puromycin and cultured in RPMI 1640 medium containing 20 % (v/v) FBS, 2 mM glutamine, 100 units/ml penicillin, 100 μg/ml streptomycin and 2 μg/ml puromycin to maintain selection for the expression plasmid. SH-SY5Y-APP cells were differentiated to generate a neuronal phenotype using 10 μM all-*trans*-retinoic acid (R2625; Sigma) for 7 days as previously described [36]. Cells were treated with GSL inhibitors, MAPK inhibitors or DAPT as indicated for up to 48 h. These compounds were added to cells in complete growth medium containing 10 % (v/v) FBS.

MTT [3-(4,5-dimethylthiazol-2-yl)-2,5-2*H*-tetrazolium bromide] cell viability assay

Cells were grown in 96-well plates (5000 cells/well) and maintained as described above. Cytotoxicity was assessed by incubating cells in 100 μl of medium containing various concentrations of GSL inhibitors as indicated along with vehicle controls (six wells per concentration). After 48 h the culture medium was removed, and 100 μl of medium [DMEM (Dulbecco's modified Eagle's medium) and 10 % (v/v) FBS] containing 0.5 mg/ml MTT (M2128; Sigma) was added and the cells were incubated for 1 h at 37 °C. The medium was discarded, and the cells were dissolved in DMSO (100 μl per well) and the absorbance of the cell lysates was measured at 550 nm. Higher absorbace values indicate increased cell viability.

Quantification of Aβ40 and Aβ42 by ELISA

Cell culture medium was collected from CHO-APP and SH-SY5Y-APP cells and pre-diluted into PBS at 1:100 for Aβ40 and at 1:10 for Aβ42 in preparation for Aβ measurement by ELISA. βMark X-40 and X-42 ELISA kits (SIG-38956-Kit and SIG-38954-Kit; Covance) were used to quantify Aβ concentration, according to the manufacturer's instructions as described previously [37].

Western blotting

Cells were routinely cultured in 12-well plates, rinsed with ice-cold PBS and lysed in lysis buffer (20 mM Tris/HCl, pH 7.5, 150 mM NaCl, 1 mM EDTA, 1 % Nonidet P40, 0.5 % deoxycholate, 0.1 % SDS and protease and phosphatase inhibitors). Bicinchoninic acid protein assays were performed on lysates and equal amounts of protein were separated by SDS/PAGE (12 % gels) and transferred on to 0.2 μm nitrocellulose membranes at 70 V for 20 min. Membranes were blocked at 22 °C for 2 h in PBS containing non-fat dried skimmed milk powder and probed with the relevant antibodies at 4 °C for 16 h to analyse APP using W0-2 monoclonal antibody [34]. The W0-2 antibody recognizes an epitope between residues 2 and 8 at the N-terminal of the Aβ peptide sequence [38,39]. ERK signalling was assessed by Western blotting using phospho-p44/42 MAPK [pERK1/2 (phosphorylated ERK 1/2)] and p44/42 MAPK (ERK1/2) rabbit monoclonal antibodies at 1:5000 dilution (#4377 and #4695 respectively; Cell Signaling Technology). Where indicated, the membranes were stripped and re-probed for β-actin (rabbit polyclonal 1:5000; A5060; Sigma), which was used as a loading control. Western blotting of secreted sAPPα (soluble APPα fragment) and secreted Aβ peptides was carried out as described previously using W0-2 monoclonal antibody [34]. Both sAPPα and Aβ were routinely analysed in growth medium containing 10 % (v/v) FBS after 48 h incubation either with or without the treatments indicated. Signals were detected using ECL® (enhanced chemiluminescence; GE Healthcare) and X-ray films. The signal intensity was quantified using NIH ImageJ software and the data presented as a ratio relative to non-treated cells as described previously [34].

PCR

RNA was isolated from cells using TRI Reagent (T9424; Sigma) following the manufacturer's protocol. All procedures were carried out using RNase-free reagents and quantification of total RNA was done by using a NanoDrop ND-1000 spectrophotometer. RNA (5 μg) was reverse transcribed into cDNA as described previously [34,40]. Conventional PCR amplification was carried out with 30 cycles of denaturation (95 °C, 30 s), annealing (58 °C, 30 s) and extension (72 °C, 30 s), and the PCR products were visualized after electrophoresis in 1 % agarose gels. The primers used are the following: GCS (GenBank® accession number AF351131.1; cDNA sequence, 141–320, 180 bp), forward, 5′-TAGCAAG-CTCCCTGGTGTCT-3′; reverse, 5′-TTCGGGTA-TTTTCCAAGCAG-3′; and GAPDH (glyceraldehyde-3-phosphate dehydrogenase; GenBank® accession number X52123.1; cDNA sequence, 309–456, 148 bp), forward, 5′-GGAGAAGGCTGGGGCCCACT-3′; reverse, 5′-GGTGGTGCAGGACGCATTGCT-3′.

siRNA inhibition of CHO-APP cell GCS expression

Transfection of siRNA into CHO-APP cells was performed using commercially prepared siRNA duplexes (Invitrogen Stealth™). The sequence targeted by the

siRNA was selected using the BLOCK-iT RNAi designer program (www.invitrogen.com/rnai), which was found to be in close agreement with available published sequences [41–43]. RNA sequences were 5′-UUAAACUGGCAACAAAGCAUUCUGA-3′, and 5′-UCAGAAUGCUUUGUUGCCAGUUUAA-3′ (Invitrogen synthesis number AF351131_stealth_880). The siRNA was targeted to GCS (UDP-glucose ceramide glucosyltransferase, UGCG; GenBank® accession number AF351131.1; cDNA sequence, 880–824)-specific sequence 5′-TCACGTAGTTTCGTTTGACTAGTAA-3′ and a random reorganization of this sequence was used as the control siRNA 5′-GAATATGCGT-TTATACCGTGTTACT-3′. siRNA duplexes were transfected by using Lipofectamine™ RNAiMAX (13778-075; Invitrogen) by a forward transfection procedure in six-well culture plates following the manufacturer's protocol. Transfection efficiency was confirmed by substituting the siRNA with fluorescently labelled BLOCK-iT reagent, supplied with the kit, using the same transfection procedure and this confirmed >95 % transfection efficiency was achieved as assessed by fluorescence microscopy (results not shown).

Cell supernatants and lysates were collected and processed for Western blot analysis as above. RNA extraction, cDNA synthesis and quantitative real-time PCR was performed as described previously [34,40]. Briefly, real-time PCR was carried out using an Eppendorf Mastercycler® ep realplex Thermal Cycler using the fluorescent dye SYBR Green (Eppendorf). Amplification was carried out with 40 cycles of 94 °C for 15 s and 60 °C for 1 min. All gene expression was normalized to GAPDH, which served as an internal control for the quality of RNA isolated from each cell sample. Experiments were performed in triplicate and at least three samples were analysed for each treatment. The level of expression for each gene was calculated using the comparative threshold cycle value (C_t) value method using the formula $2^{-\Delta\Delta Ct}$ (where $\Delta\Delta C_t = \Delta C_t$ sample $- \Delta C_t$ reference) as described previously [44,45].

Cellular GSL analysis

GSL profiles of CHO-APP cells were analysed as described previously [24]. Briefly, cells grown to confluence in six-well plates were treated with synthetic ceramide analogues as described above, rinsed three times with PBS and lipids extracted in 2:1 (v/v) chloroform/methanol. The GSL fractions were isolated by silicic acid chromatography, and the glycan moiety was released by ceramide glycanase addition [46]. The GSL glycans were then fluorescently labelled with 2AA (2-anthranilic acid) and analysed by normal phase HPLC as described previously [24]. Total peak area units for the glycan peaks were pooled to calculate the reduction of cellular GSL levels after treatment with ceramide analogues or GCS siRNA. We noted that interfering peaks eluting in the positions of glucose and lactose were detected in the commercial ceramide glycanase enzyme blank conditions, and levels of GlcCer (glucosylceramide) and LacCer (lactosylceramide) were therefore excluded from the analyses of CHO-APP GSL levels. The principal GSLs analysed (asialo ganglioside G_{M2}, globotriaosylceramide, G_{M3} and globotetraosylceramide) were identified based on their glucose unit values by comparison with a 2-AA-labelled dextran standard as previously described in detail [46,47]. Values were expressed as a percentage of total GSL levels present in mock-treated CHO-APP cells.

Statistical analysis

Unless stated otherwise, experiments were performed in triplicate and with three experimental replicates. Results are presented as means with S.E.M. shown by error bars. Differences were considered significant where $P < 0.05$, as determined using a two-tailed Student's t test for unpaired data.

RESULTS

Previous studies have shown that PDMP inhibits Aβ production from the human SH-SY5Y neuronal cell line by ~55 % when used at a concentration of 25 μM for 48 h [10]. We recently confirmed this finding and showed that D-PDMP also inhibits Aβ production in the well-characterized CHO-APP cell line [17]. In the latter experiments, 48 h treatment of CHO-APP cells with 15 μM D-PDMP reduced Aβ levels by ~50 % and an IC_{50} value of 15.8 μM was calculated for PDMP-mediated inhibition of Aβ production [17]. Using identical experimental conditions, we assessed whether ERK phosphorylation may be modulated by D-PDMP. At a concentration of 15 μM, D-PDMP inhibited Aβ production by 44 % as predicted (Figure 1). Under these conditions, pERK levels were also reduced by 27 % with no change in total ERK (Figure 1). Since our previous studies indicated that the structurally related PDMP analogues, PPMP and EtDO-P4, were more potent anti-amyloidogenic compounds that were more likely to be useful as prototype therapeutic agents *in vivo* [17], we next assessed the impact of these compounds on cellular Aβ production and ERK activation.

Earlier studies indicated that the D-*threo*-enantiomers of PDMP and structurally related compounds represent the active forms of these GSL synthesis inhibitors [18–23]. We therefore assessed the enantiomer-specific effects of PPMP and EtDO-P4 on both Aβ production and ERK activation. Consistent with previous data [17], 5 μM D-PPMP inhibited Aβ production by 49 %, whereas L-PPMP had no effect at the same concentration (Figure 2). Cellular APP and secreted sAPPα were unaffected by these compounds (Figure 2). In contrast, both D- and

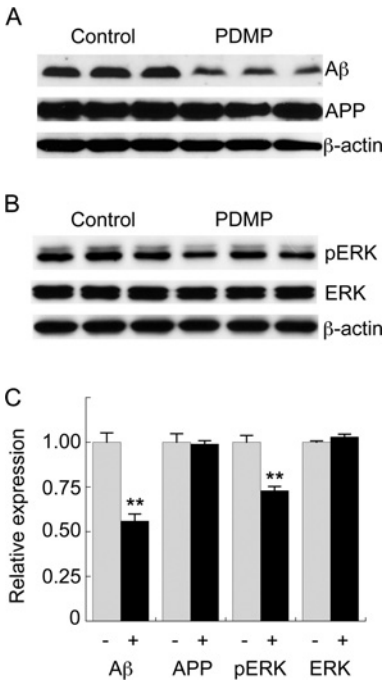

Figure 1 PDMP reduces Aβ production and reduces phosphorylation of ERK

CHO-APP cells were treated with 15 μM PDMP for 48 h. Secreted Aβ and cellular APP (A), and total ERK and pERK (B) were measured by Western blotting. β-Actin was used as a loading control. Absorbance measurements of the blots are shown in the histogram (C); grey bars, control; black bars, treated. Results are mean ± S.E.M. values; $^{**}P < 0.01$.

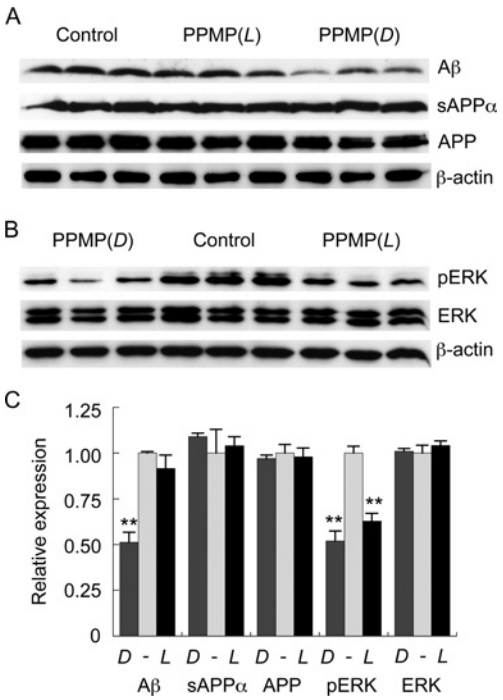

Figure 2 PPMP D-enantiomer reduces Aβ production and ERK phosphorylation, whereas PPMP L-enantiomer reduces ERK phosphorylation without affecting Aβ production

CHO-APP cells were treated with 5 μM D- or L-PPMP for 48 h. Secreted Aβ and sAPPα and cellular APP (A) and total ERK and pERK (B) were measured by Western blotting. β-Actin was used as a loading control. Absorbance measurements of the blots are shown in the histogram (C); grey bars, control; dark grey bars, D-PPMP treated; and black bars: L-PPMP. Results are mean ± S.E.M. values; $^{**}P < 0.01$.

L-PPMP significantly inhibited ERK phosphorylation (Figure 2). Similarly, when we assessed the D- and L-*threo* enantiomers of EtDO-P4 at a concentration of 1 μM, only the D-EtDO-P4 (which was the more potent GSL synthesis inhibitor) significantly inhibited Aβ production, whereas both D- and L-EtDO-P4 inhibited ERK phosphorylation (Figure 3). Unexpectedly, the L-EtDO-P4 that we separated from the D/L-EtDO-P4 mixture by preparative chiral HPLC (results not shown) also reduced cellular GSL levels by 43 % (Figure 3A). Even though the inhibition of Aβ production by the D-enantiomers of all three ceramide analogues (PDMP, PPMP and EtDO-P4) occurred concomitantly with inhibition of ERK phosphorylation, this is unlikely to represent their primary mode of anti-amyloidogenic action since the L-enantiomers also inhibited ERK activation without significantly reducing Aβ production. It was also intriguing that the L-EtDO-P4-mediated reductions in cellular GSL levels (which were less pronounced than the GSL reduction resulting from D-EtDO-P4) did not significantly reduce Aβ production.

To rule out the possibility that the enantiomer-specific effect of PPMP on cellular Aβ production was simply due to the concentration used, various concentrations of both D-PPMP and L-PPMP were tested in parallel. Since these compounds can become cytotoxic at high concentrations, we first determined cell viability at various inhibitor doses using the MTT assay. Consistent with our previous data [17], cells remained ~85 % viable after 48 h treatment with 5 μM D-PPMP (Figure 4A). Increased toxicity was detected when the concentration of the inhibitor was raised to 10 μM or above (Figure 4A). At PPMP concentrations above 10 μM, cells also began to detach from the plates and therefore data pertaining to MTT reduction and Aβ levels at 15 μM are not quantitative and are therefore not presented herein. The cytotoxicity profiles of both the D- and L-isomers in the 1–10 μM range were very similar (Figure 4A). Importantly, D-PPMP dose-dependently inhibited Aβ generation, whereas L-PPMP did not (Figure 4). The levels of another W0-2-positive protein of unknown identity at a molecular mass of ~15 kDa did not change with inhibitor treatment in the 1–10 μM range, suggesting that the impact of D-PPMP is not a generalized action on cellular protein production.

We next investigated the enantiomer-specific inhibition of cellular Aβ production in the SH-SY5Y-APP neuronal

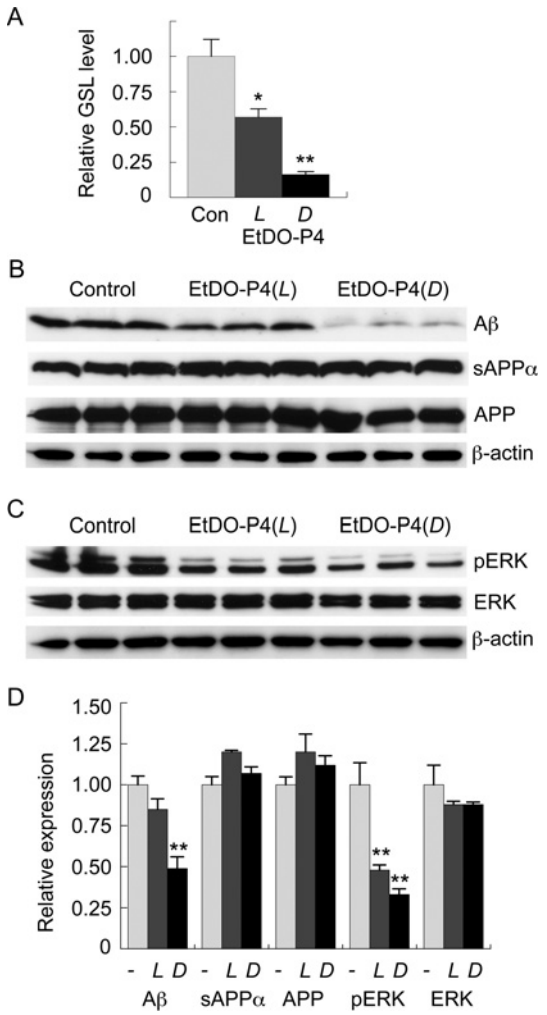

Figure 3 Effect of EtDO-P4 enantiomers on GSL synthesis, Aβ production and ERK phosphorylation

CHO-APP cells were treated with 1 μM D-EtDO-P4 or L-EtDO-P4 enantiomer for 48 h. Lipids were extracted and GSL-derived glycans were analysed by normal phase HPLC (A). Secreted Aβ and sAPPα and cellular APP (B) and total ERK and pERK (C) were analysed by Western blotting. β-Actin was used as a loading control. Absrobance measurements of the blots are shown in the histogram (C). Grey bars, control; dark grey bars, EtDO-P4 L-enantiomer; black bars, EtDO-P4 D-enantiomer. Results are mean $\pm$ S.E.M. values; $^{*}P < 0.05$, $^{**}P < 0.01$.

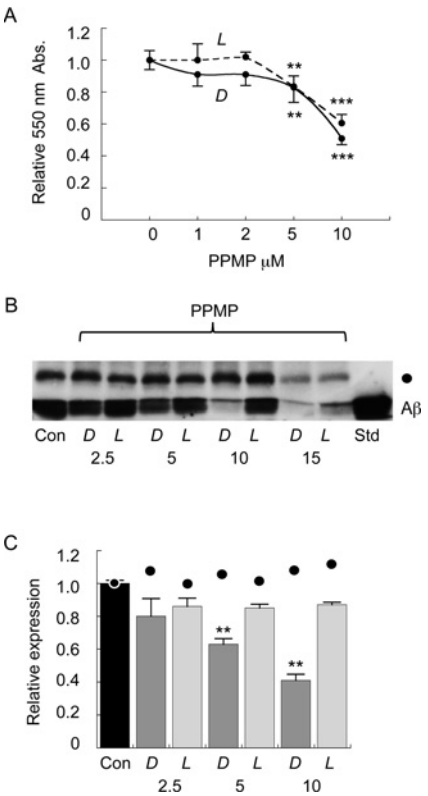

Figure 4 Dose-dependent effect of PPMP enantiomers on cellular viability and Aβ secretion by CHO-APP cells

CHO-APP cells were treated with D- and L-PPMP for 48 h at the indicated concentrations (μM). Cytotoxicity was determined by MTT reduction and the data were normalized to a control value set at 1.0 (A). The broken line indicates L-PPMP ('L') and the solid line indicates D-PPMP ('D'). Data are not included for doses of 15 μM and above due to cell loss from the wells. Cell culture supernatants were also assessed for secreted Aβ after treatment with 2.5, 5, 10 and 15 μM PPMP (B). Synthetic Aβ40 peptide (1 ng) was added as an additional marker protein ('Std'). An uncharacterized secreted W0-2-positive band at $\sim$15 kDa (●) is also shown for the purposes of comparison as secretion of this protein is not affected by either PPMP enantiomer at levels (1–10 μM) that do not result in cell loss. Absorbance measurements of the Western blots carried out in triplicate are shown in the histogram (C). Black bar, control; dark grey bars, D-PPMP treated; and grey bars, L-PPMP. Results are mean $\pm$ S.E.M. values; $^{**}P < 0.01$. The mean relative levels of the uncharacterized 15 kDa W0-2-positive band are indicated by (●).

cell line. Both D-PPMP and L-PPMP displayed similar cytotoxicity profiles in the neuronal cells as compared with the CHO-APP cells (Figure 5A; cf Figure 4A). In the neuronal cell line viability remained at $\sim$90% at inhibitor concentrations of 5 μM (Figure 5A). Furthermore, only the D-enantiomer inhibited Aβ production, whereas both the D- and L-enantiomers inhibited ERK phosphorylation (Figure 5). In order to determine if D-PPMP selectively inhibits either Aβ40 or Aβ42 production, we used an ELISA to quantify these species. This indicated that the CHO-APP cell line generates 7.5-fold more Aβ40 and 8.1-fold more Aβ42 than the SH-SY5Y cell lines and that in both cases the amount of Aβ40 produced was $\sim$15-fold higher than Aβ42 (Figure 6). Subsequent to treatment with 5 μM D-PPMP, production of Aβ40 was reduced by 74 and 81% in the CHO-APP and SH-SY5Y-APP cell lines respectively, whereas Aβ42 was reduced by 38% but only in CHO-APP cells (Figure 6). This indicates that the reduction in Aβ is predominantly due to reduction in Aβ40. There were no significant reductions in Aβ when cells were treated with L-PPMP and the ELISA data are

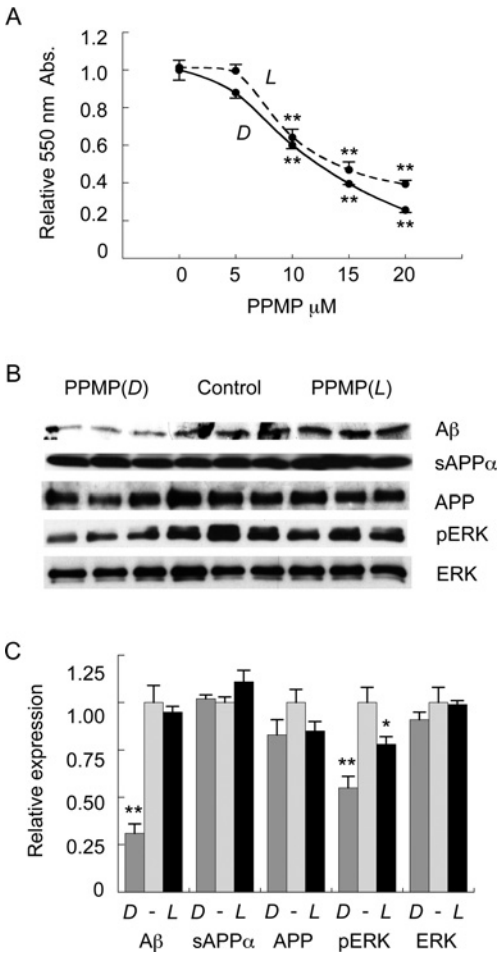

Figure 5 PPMP D-enantiomer reduces neuronal Aβ production and ERK phosphorylation, whereas PPMP L-enantiomer reduces ERK phosphorylation without affecting Aβ production

SH-SY5Y-APP cells were treated with D- and L-PPMP for 48 h at the indicated concentrations (μM), the cytotoxicity was determined by the MTT reduction assay and the data were normalized to a control value set at 1.0 (A). The broken line indicates L-PPMP ('L'), and the solid line indicates D-PPMP ('D'). SH-SY5Y-APP cells were treated with 5 μM D- or L-PPMP for 48 h. Secreted Aβ and sAPPα, cellular APP and total ERK and pERK were measured by Western blotting (B). Absorbance measurements of the blots are shown in the histogram (C); '-' grey bars, control; dark grey bars, D-PPMP treated; and black bars, L-PPMP. Results are mean ± S.E.M. values; $^{*}P < 0.05$, $^{**}P < 0.01$.

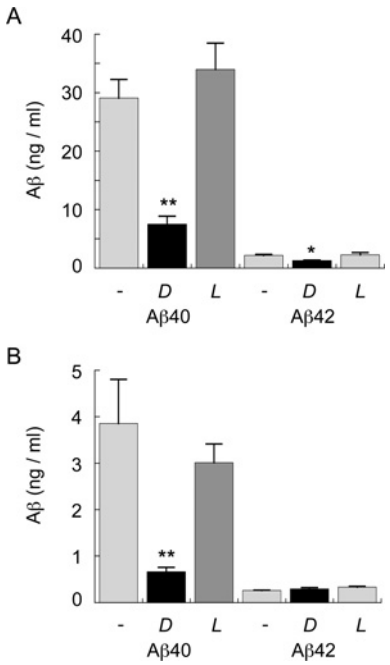

Figure 6 Quantification of Aβ40 and Aβ42 species in CHO-APP (A) and SH-SY5Y-APP (B) cell culture supernatants

Cells were treated with 5 μM PPMP enantiomers as indicated for 48 h and the medium was assessed for Aβ40 and Aβ42 by ELISA. Experiments were performed in triplicate and each sample was assayed in duplicate. The concentrations of Aβ40 and Aβ42 (ng/ml) are shown in the histograms; '-' light-grey bars, control; black bars, D-PPMP treated; dark-grey bars, L-PPMP treated. Results are mean ± S.E.M. values; $^{*}P < 0.05$, $^{**}P < 0.01$.

therefore in good agreement with the semi-quantitative Western blot analysis.

Taken together, these experiments raise two important issues regarding: (i) the direct role that ERK activation may play in amyloidogenic APP processing and (ii) the specificity of reduced cellular GSL synthesis as a modulator of Aβ production. These issues were addressed using alternative approaches to inhibit ERK phosphorylation or GSL synthesis. To probe for a direct role that ERK signalling may play in Aβ production, CHO-APP cells were treated with two different well-characterized MAPK pathway inhibitors, PD98059 or U0126. Both PD98059 and U0126 strongly inhibited pERK formation; however, Aβ production was not suppressed (Figure 7). In fact, for reasons that remain unknown, PD98059 stimulated Aβ production by 20% (Figure 7). The results from these experiments further suggest that the inhibition of ERK activation by PDMP, PPMP and EtDO-P4 is not likely to underlie their actions as inhibitors of cellular Aβ production.

In a final set of experiments we assessed the impact that inhibition of GSL synthesis using siRNA has on both cellular Aβ production and ERK phosphorylation. Targeting of GCS using a 40 nM concentration of siRNA duplex for 48 h reduced GCS mRNA levels by 82% (Figure 8). This resulted in a 77% decrease in CHO-APP cellular GSL levels (Figure 8). The relative reductions in the levels of the different GSL species were similar when either ceramide analogues (see Supplementary Figure S1 at http://www.clinsci.org/cs/122/cs1220409add.htm) or siRNA (Figure 8) was used to inhibit GCS. In parallel experiments, GCS siRNA treatment of CHO-APP cells did not result in any detectable changes in either Aβ production or ERK phosphorylation (Figure 9). These data indicate that reductions in cellular GSL levels alone are not sufficient to reduce cellular Aβ production.

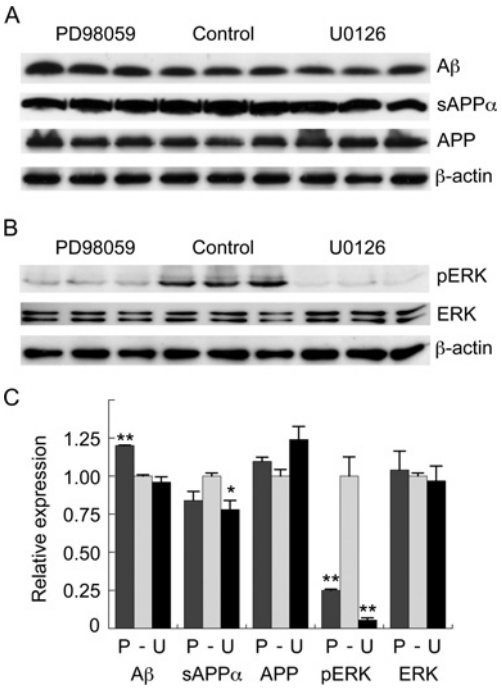

Figure 7 Specific inhibition of ERK phosphorylation does not reduce Aβ production

CHO-APP cells were treated with specific ERK phosphorylation inhibitors PD98059 (10 μM) or U0126 (5 μM). Secreted Aβ and sAPPα and cellular APP (A) and total ERK and pERK (B) were analysed by Western blotting. β-Actin was used as a loading control. Absorbance measurements of the Western blots are shown in the histogram (C): grey bars, control; dark grey bars, PD98059 treated; black bars, U0126 treated. Results are mean $\pm$ S.E.M. values; $^{*}P < 0.05$, $^{**}P < 0.01$.

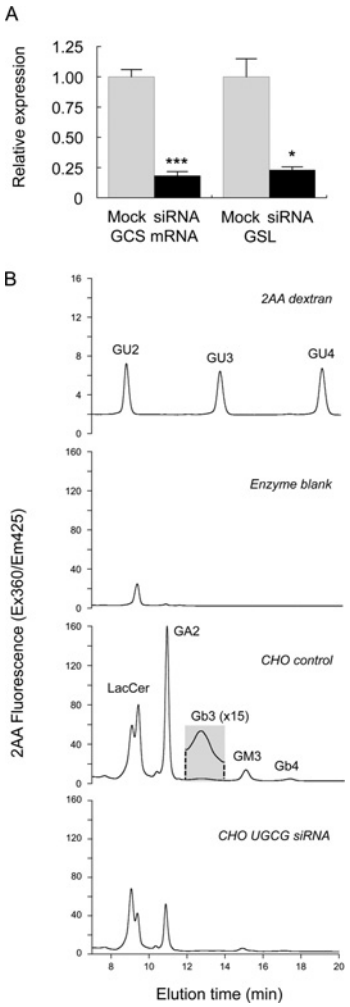

Figure 8 siRNA knockdown of GCS reduces CHO-APP cellular GSL levels

CHO-APP cells were transfected with GCS siRNA duplex (40 nM) or scrambled siRNA for 48 h. RNA and lipids were extracted from replicate cell culture plates for real-time PCR and HPLC analyses. Relative expression data for both CGS mRNA and cellular GSL levels are shown in the histogram (A); grey bars, scrambled siRNA; black bars, GCS siRNA. Results mean $\pm$ S.E.M. values ($n = 3$); $^{*}P < 0.05$, $^{***}P < 0.001$. Representative HPLC chromatograms are shown (B). The dextran ladder '2AA dextran' was used to calculate glucose unit (GU) values and thus identify the cellular GSL species. The enzyme blank samples 'Enzyme blank' indicate the presence of a contaminating peak in the position of LacCer. The lower two chromatograms indicate HPLC separation of glycans from mock and GCS siRNA-treated samples. Note that the *y*-axis for the globotriaosylceramide peak is expanded 15 times to allow visualization. GA2, asialo ganglioside G_{M2}; Gb3, globotriaosylceramide; Gb4, globotetraosylceramide; GM3, ganglioside G_{M3}.

DISCUSSION

There is accumulating data to suggest that alterations in cerebral lipid homoeostasis may be directly associated with AD (see [48] for a review). Based on the fact that APP is a type I membrane protein that is proteolytically processed to form Aβ in sphingolipid-enriched membrane microdomains, the possibility that modulation of membrane lipid composition could represent a novel means to regulate Aβ production presents a plausible basis for AD therapeutic intervention [9,11,49–52].

Studies from different laboratories have shown that the ceramide analogue inhibitors of GCS that are based on the PDMP structure inhibit Aβ production *in vitro* [10,17]; however, the mechanism(s) of their anti-amyloidogenic action remain to be fully elucidated. In the present studies, we have shown that the inhibition of ERK phosphorylation mediated by these GSL inhibitors is not likely to contribute to their anti-amyloidogenic actions since both D- and L-enantiomers inhibit ERK activation, whereas only the D-enantiomers suppress cellular Aβ production. It remains possible that the efficacy of additional anti-amyloidogenic compounds is related to modulation of the ERK pathway, and in associated studies (see Supplementary Figure S2 at http://www.clinsci.org/cs/122/cs1220409add.htm) we found that the inhibition of Aβ production by lovastatin [a competitive inhibitor of HMG-CoA (3-hydroxy-3-methylglutaryl-CoA) reductase (a cholesterol-lowering drug)] was correlated with reduced ERK

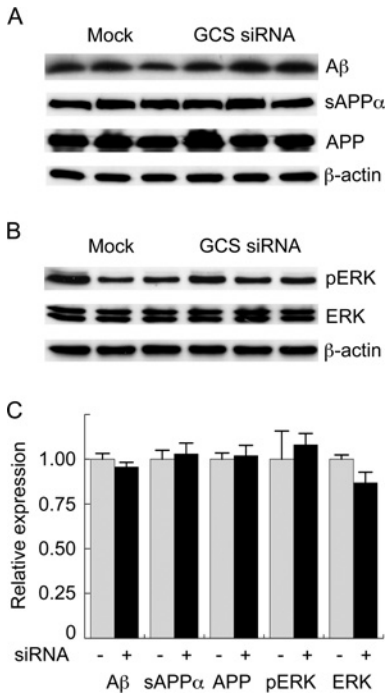

Figure 9 Endogenous GCS knockdown has little impact on Aβ production and ERK phosphorylation

CHO-APP cells were transfected with GCS siRNA duplex (40 nM) or scrambled siRNA for 48 h. Secreted Aβ and sAPPα and cellular APP (A) and total ERK and pERK (B) were measured by Western blotting with β-actin used as a loading control. Absorbance measurements of the Western blots are shown in the histogram (C); grey bars, control; black bars, GCS-siRNA. Results are mean $\pm$ S.E.M. values.

phosphorylation (whereas the γ-secretase inhibitor DAPT did not alter ERK signalling). Since ERK signalling is clearly dysregulated in AD [28,29], normalization of this pathway may still represent a therapeutic option (for PDMP-related compounds and other more specific ERK modulators), however, this does not appear to be the pathway by which these ceramide analogues inhibit Aβ production.

A recent study indicates that inhibition of the ERK pathway has no impact on cellular sAPPα secretion [53]. This finding is in agreement with the present study that shows inhibition of ERK activation by PDMP, PPMP and EtDO-P4, and their enantiomers, where applicable, does not significantly alter cellular sAPPα secretion. It is noteworthy, however, that some aspects of α-secretase activity may be modulated by ERK activation in a substrate-specific manner as ERK1 does control α-secretase-mediated processing of the cellular prion protein [54].

Previous research suggests that raft-associated GSLs promote amyloidogenic processing of APP via regulation of BACE and γ-secretase activities [9,11]. We therefore speculated that the inhibition of Aβ production by the ceramide analogue GCS inhibitors we used would be mirrored by siRNA silencing of GCS. Intriguingly, the $\sim$75% reduction in cellular GSL levels that was induced by GCS knockdown had no impact on Aβ production. This may indicate that the D-enantiomers of the ceramide analogues we have used have additional actions (either direct or indirect) on APP processing that remain to be discovered and that inhibition of GSL synthesis alone (i.e. using siRNA targeting) may only be efficacious in situations where membrane GSL levels are increased above their physiological concentrations. Alternatively, it may be that modulation of very specific neutral or charged GSL species that are not highly expressed in the *in vitro* systems we have used is required to reveal an impact on Aβ production. Future studies would be required to examine the effect that the numerous individual GSL species may have on cellular APP processing. We acknowledge that specific GSLs play other roles (in addition to potentially regulating APP processing) that may impact on AD pathology. As a case in point, ganglioside G_{M1} plays a crucial role in regulating the transition of monomeric Aβ to neurotoxic oligomers and the use of compounds such as D-EtDO-P4 to suppress this activity would represent a viable therapeutic target that is independent of its impact on APP processing.

It is noteworthy that D-*threo*-EtDO-P4 has been administered successfully in long-term studies in mice [21,55]. In addition, a potentially relevant GCS inhibitor {Eliglustat tartrate, (1R,2R)-octanoic acid [2-(2′,3′-dihydro-benzo [1,4] dioxin-6′-yl)-2-hydroxy-1-pyrrolidin-1-ylmethyl-ethyl]-amide-L-tartaric acid salt, formerly Genz-112638} is currently in human clinical trials to treat Type 1 Gaucher disease where it has been shown to reduce plasma GlcCer and G_{M3} levels in association with improvement in a number of clinical manifestations of the disease [56–59]. The data from our group and others suggest that such GCS inhibitors may also be worth investigating as anti-amyloidogenic agents in relevant AD amyloidogenic mouse models and potentially in the human AD setting.

AUTHOR CONTRIBUTION

Hongyun Li conducted the experimental work with contributions from Ya Hui Hung and Brett Garner. Hongyun Li, Genevieve Evin, Andrew Hill, Ashley Bush and Brett Garner contributed to method development, establishment of cell lines, experimental design and data interpretation. Hongyun Li and Brett Garner wrote the paper with contributions from Genevieve Evin, Andrew Hill, Ya Hui Hung and Ashley Bush.

ACKNOWLEDGEMENTS

We are grateful to Professor Colin Masters and Dr Qiao-Xin Li for providing the W0-2 antibody, and to Michael Ho for maintaining the SH-SY5Y-APP cell line.

FUNDING

This work was supported by the Australian National Health and Medical Research Council [project grant number 568651]. B.G. is supported by a fellowship from the Australian Research Council (ARC Future Fellowship) [grant number FT0991986].

REFERENCES

1 Braak, H. and Braak, E. (1991) Neuropathological stageing of Alzheimer-related changes. Acta. Neuropathol. **82**, 239–259
2 Kang, J., Lemaire, H. G., Unterbeck, A., Salbaum, J. M., Masters, C. L., Grzeschik, K. H., Multhaup, G., Beyreuther, K. and Muller-Hill, B. (1987) The precursor of Alzheimer's disease amyloid A4 protein resembles a cell-surface receptor. Nature **325**, 733–736
3 Selkoe, D. J. (2001) Alzheimer's disease: genes, proteins, and therapy. Physiol. Rev. **81**, 741–766
4 Kerr, M. L. and Small, D. H. (2005) Cytoplasmic domain of the β-amyloid protein precursor of Alzheimer's disease: function, regulation of proteolysis, and implications for drug development. J. Neurosci. Res. **80**, 151–159
5 Ward, R. V., Jennings, K. H., Jepras, R., Neville, W., Owen, D. E., Hawkins, J., Christie, G., Davis, J. B., George, A., Karran, E. H. and Howlett, D. R. (2000) Fractionation and characterization of oligomeric, protofibrillar and fibrillar forms of β-amyloid peptide. Biochem. J. **348**, 137–144
6 Hung, L. W., Ciccotosto, G. D., Giannakis, E., Tew, D. J., Perez, K., Masters, C. L., Cappai, R., Wade, J. D. and Barnham, K. J. (2008) Amyloid-β peptide (Aβ) neurotoxicity is modulated by the rate of peptide aggregation: Aβ dimers and trimers correlate with neurotoxicity. J. Neurosci. **28**, 11950–11958
7 Evin, G., Sernee, M. F. and Masters, C. L. (2006) Inhibition of γ-secretase as a therapeutic intervention for Alzheimer's disease: prospects, limitations and strategies. CNS Drugs **20**, 351–372
8 Yanagisawa, K., Odaka, A., Suzuki, N. and Ihara, Y. (1995) GM1 ganglioside-bound amyloid β-protein (Aβ): a possible form of preamyloid in Alzheimer's disease. Nat. Med. **1**, 1062–1066
9 Kalvodova, L., Kahya, N., Schwille, P., Ehehalt, R., Verkade, P., Drechsel, D. and Simons, K. (2005) Lipids as modulators of proteolytic activity of BACE: involvement of cholesterol, glycosphingolipids, and anionic phospholipids *in vitro*. J. Biol. Chem. **280**, 36815–36823
10 Tamboli, I. Y., Prager, K., Barth, E., Heneka, M., Sandhoff, K. and Walter, J. (2005) Inhibition of glycosphingolipid biosynthesis reduces secretion of the β-amyloid precursor protein and amyloid β-peptide. J. Biol. Chem. **280**, 28110–28117
11 Osenkowski, P., Ye, W., Wang, R., Wolfe, M. S. and Selkoe, D. J. (2008) Direct and potent regulation of γ-secretase by its lipid microenvironment. J. Biol. Chem. **283**, 22529–22540
12 Yahi, N., Aulas, A. and Fantini, J. (2010) How cholesterol constrains glycolipid conformation for optimal recognition of Alzheimer's β amyloid peptide (Aβ1–40). PLoS ONE **5**, e9079
13 Tamboli, I. Y., Hampel, H., Tien, N. T., Tolksdorf, K., Breiden, B., Mathews, P. M., Saftig, P., Sandhoff, K. and Walter, J. (2011) Sphingolipid storage affects autophagic metabolism of the amyloid precursor protein and promotes Aβ generation. J. Neurosci. **31**, 1837–1849
14 Hayashi, H., Kimura, N., Yamaguchi, H., Hasegawa, K., Yokoseki, T., Shibata, M., Yamamoto, N., Michikawa, M., Yoshikawa, Y., Terao, K. et al. (2004) A seed for Alzheimer amyloid in the brain. J. Neurosci. **24**, 4894–4902
15 Martins, I. C., Kuperstein, I., Wilkinson, H., Maes, E., Vanbrabant, M., Jonckheere, W., Van Gelder, P., Hartmann, D., D'Hooge, R., De Strooper, B. et al. (2008) Lipids revert inert Aβ amyloid fibrils to neurotoxic protofibrils that affect learning in mice. EMBO J. **27**, 224–233
16 Bernardo, A., Harrison, F. E., McCord, M., Zhao, J., Bruchey, A., Davies, S. S., Jackson Roberts, II, L., Mathews, P. M., Matsuoka, Y., Ariga, T. et al. (2009) Elimination of GD3 synthase improves memory and reduces amyloid-β plaque load in transgenic mice. Neurobiol. Aging **30**, 1777–1791
17 Li, H., Kim, W. S., Guilemin, G. J., Hill, A. F., Evin, G. and Garner, B. (2010) Modulation of amyloid precursor protein processing by synthetic ceramide analogues. Biochim. Biophys. Acta **1801**, 887–895
18 Abe, A., Radin, N. S., Shayman, J. A., Wotring, L. L., Zipkin, R. E., Sivakumar, R., Ruggieri, J. M., Carson, K. G. and Ganem, B. (1995) Structural and stereochemical studies of potent inhibitors of glucosylceramide synthase and tumor cell growth. J. Lipid Res. **36**, 611–621
19 Basu, M., Girzadas, M., Dastgheib, S., Baker, J., Rossi, F., Radin, N. S. and Basu, S. (1997) Ceramide glycanase from rat mammary tissues: inhibition by PPMP(D-/L-) and its probable role in signal transduction. Indian J. Biochem. Biophys. **34**, 142–149
20 Lee, L., Abe, A. and Shayman, J. A. (1999) Improved inhibitors of glucosylceramide synthase. J. Biol. Chem. **274**, 14662–14669
21 Abe, A., Gregory, S., Lee, L., Killen, P. D., Brady, R. O., Kulkarni, A. and Shayman, J. A. (2000) Reduction of globotriaosylceramide in Fabry disease mice by substrate deprivation. J. Clin. Invest. **105**, 1563–1571
22 Shayman, J. A., Lee, L., Abe, A. and Shu, L. (2000) Inhibitors of glucosylceramide synthase. Methods Enzymol. **311**, 373–387
23 Abe, A., Wild, S. R., Lee, W. L. and Shayman, J. A. (2001) Agents for the treatment of glycosphingolipid storage disorders. Curr. Drug Metab. **2**, 331–338
24 Glaros, E. N., Kim, W. S., Quinn, C. M., Wong, J., Gelissen, I., Jessup, W. and Garner, B. (2005) Glycosphingolipid accumulation inhibits cholesterol efflux via the ABCA1/apoA-I pathway. 1-Phenyl-2-decanoylamino-3-morpholino-1-propanol is a novel cholesterol efflux accelerator. J. Biol. Chem. **280**, 24515–24523
25 Odintsova, E., Butters, T. D., Monti, E., Sprong, H., van Meer, G. and Berditchevski, F. (2006) Gangliosides play an important role in the organization of CD82-enriched microdomains. Biochem. J. **400**, 315–325
26 Yanagisawa, M., Nakamura, K. and Taga, T. (2005) Glycosphingolipid synthesis inhibitor represses cytokine-induced activation of the Ras-MAPK pathway in embryonic neural precursor cells. J. Biochem. **138**, 285–291
27 Hyman, B. T., Elvhage, T. E. and Reiter, J. (1994) Extracellular signal regulated kinases. Localization of protein and mRNA in the human hippocampal formation in Alzheimer's disease. Am. J. Pathol. **144**, 565–572
28 McShea, A., Zelasko, D. A., Gerst, J. L. and Smith, M. A. (1999) Signal transduction abnormalities in Alzheimer's disease: evidence of a pathogenic stimuli. Brain Res. **815**, 237–242
29 Zhu, X., Sun, Z., Lee, H. G., Siedlak, S. L., Perry, G. and Smith, M. A. (2003) Distribution, levels, and activation of MEK1 in Alzheimer's disease. J. Neurochem. **86**, 136–142
30 Mills, J., Laurent Charest, D., Lam, F., Beyreuther, K., Ida, N., Pelech, S. L. and Reiner, P. B. (1997) Regulation of amyloid precursor protein catabolism involves the mitogen-activated protein kinase signal transduction pathway. J. Neurosci. **17**, 9415–9422
31 Desdouits-Magnen, J., Desdouits, F., Takeda, S., Syu, L. J., Saltiel, A. R., Buxbaum, J. D., Czernik, A. J., Nairn, A. C. and Greengard, P. (1998) Regulation of secretion of Alzheimer amyloid precursor protein by the mitogen-activated protein kinase cascade. J. Neurochem. **70**, 524–530
32 Sodhi, C. P., Perez, R. G. and Gottardi-Littell, N. R. (2008) Phosphorylation of β-amyloid precursor protein (APP) cytoplasmic tail facilitates amyloidogenic processing during apoptosis. Brain Res. **1198**, 204–212
33 White, A. L., Guerra, B., Wang, J. and Lanford, R. E. (1999) Presecretory degradation of apolipoprotein. J. Lipid Res. **40**, 275–286

34 Kim, W. S., Suryo Rahmanto, A., Kamili, A., Rye, K. A., Guillemin, G. J., Gelissen, I. C., Jessup, W., Hill, A. F. and Garner, B. (2007) Role of ABCG1 and ABCA1 in regulation of neuronal cholesterol efflux to apolipoprotein-E discs and suppression of amyloid-β peptide generation. J. Biol. Chem. **282**, 2851–2861

35 Hung, Y. H., Robb, E. L., Volitakis, I., Ho, M., Evin, G., Li, Q. X., Culvenor, J. G., Masters, C. L., Cherny, R. A. and Bush, A. I. (2009) Paradoxical condensation of copper with elevated β-amyloid in lipid rafts under cellular copper deficiency conditions: implications for Alzheimer disease. J. Biol. Chem. **284**, 21899–21907

36 Cheung, Y. T., Lau, W. K., Yu, M. S., Lai, C. S., Yeung, S. C., So, K. F. and Chang, R. C. (2009) Effects of all-trans-retinoic acid on human SH-SY5Y neuroblastoma as *in vitro* model in neurotoxicity research. Neurotoxicology **30**, 127–135

37 Elliott, D. A., Tsoi, K., Holinkova, S., Chan, S. L., Kim, W. S., Halliday, G. M., Rye, K. A. and Garner, B. (2011) Isoform-specific proteolysis of apolipoprotein-E in the brain. Neurobiol. Aging **32**, 257–271

38 Ida, N., Hartmann, T., Pantel, J., Schroder, J., Zerfass, R., Forstl, H., Sandbrink, R., Masters, C. L. and Beyreuther, K. (1996) Analysis of heterogeneous A4 peptides in human cerebrospinal fluid and blood by a newly developed sensitive Western blot assay. J. Biol. Chem. **271**, 22908–22914

39 Miles, L. A., Wun, K. S., Crespi, G. A., Fodero-Tavoletti, M. T., Galatis, D., Bagley, C. J., Beyreuther, K., Masters, C. L., Cappai, R., McKinstry, W. J. et al. (2008) Amyloid-β-anti-amyloid-β complex structure reveals an extended conformation in the immunodominant B-cell epitope. J. Mol. Biol. **377**, 181–192

40 Kim, W. S., Guillemin, G. J., Glaros, E. N., Lim, C. K. and Garner, B. (2006) Quantitation of ATP-binding cassette subfamily-A transporter gene expression in primary human brain cells. NeuroReport **17**, 891–896

41 Saito, M., Fukushima, Y., Tatsumi, K., Bei, L., Fujiki, Y., Iwamori, M., Igarashi, T. and Sakakihara, Y. (2002) Molecular cloning of Chinese hamster ceramide glucosyltransferase and its enhanced expression in peroxisome-defective mutant Z65 cells. Arch. Biochem. Biophys. **403**, 171–178

42 Diaz-Font, A., Chabas, A., Grinberg, D. and Vilageliu, L. (2006) RNAi-mediated inhibition of the glucosylceramide synthase (GCS) gene: A preliminary study towards a therapeutic strategy for Gaucher disease and other glycosphingolipid storage diseases. Blood Cells Mol. Dis. **37**, 197–203

43 D'Angelo, G., Polishchuk, E., Di Tullio, G., Santoro, M., Di Campli, A., Godi, A., West, G., Bielawski, J., Chuang, C. C., van der Spoel, A. C. et al. (2007) Glycosphingolipid synthesis requires FAPP2 transfer of glucosylceramide. Nature **449**, 62–67

44 Cheng, A., Johnson, C. L. and Ford, L. P. (2008) A step-by-step procedure to analyze the efficacy of siRNA using real-time PCR. Methods Mol. Biol. **419**, 303–316

45 Livak, K. J. and Schmittgen, T. D. (2001) Analysis of relative gene expression data using real-time quantitative PCR and the $2^{-\Delta\Delta C(T)}$. Method. Methods **25**, 402–408

46 Wing, D. R., Garner, B., Hunnam, V., Reinkensmeier, G., Andersson, U., Harvey, D. J., Dwek, R. A., Platt, F. M. and Butters, T. D. (2001) High-performance liquid chromatography analysis of ganglioside carbohydrates at the pmol level after ceramide glycanse digestion and fluorescent labelling with 2-aminobenzamide. Anal. Biochem. **298**, 207–217

47 Neville, D. C., Coquard, V., Priestman, D. A., te Vruchte, D. J., Sillence, D. J., Dwek, R. A., Platt, F. M. and Butters, T. D. (2004) Analysis of fluorescently labeled glycosphingolipid-derived oligosaccharides following ceramide glycanase digestion and anthranilic acid labeling. Anal. Biochem. **331**, 275–282

48 Garner, B. (2010) Lipids and Alzheimer's disease. Biochim. Biophys. Acta **1801**, 747–749

49 Ehehalt, R., Keller, P., Haass, C., Thiele, C. and Simons, K. (2003) Amyloidogenic processing of the Alzheimer β-amyloid precursor protein depends on lipid rafts. J. Cell Biol. **160**, 113–123

50 Lusa, S., Blom, T. S., Eskelinen, E. L., Kuismanen, E., Mansson, J. E., Simons, K. and Ikonen, E. (2001) Depletion of rafts in late endocytic membranes is controlled by NPC1-dependent recycling of cholesterol to the plasma membrane. J. Cell Sci. **114**, 1893–1900

51 Simons, M., Keller, P., De Strooper, B., Beyreuther, K., Dotti, C. G. and Simons, K. (1998) Cholesterol depletion inhibits the generation of β-amyloid in hippocampal neurons. Proc. Natl. Acad. Sci. U.S.A. **95**, 6460–6464

52 Haughey, N. J., Bandaru, V. V., Bae, M. and Mattson, M. P. (2010) Roles for dysfunctional sphingolipid metabolism in Alzheimer's disease neuropathogenesis. Biochim. Biophys. Acta **1801**, 878–886

53 Cisse, M., Braun, U., Leitges, M., Fisher, A., Pages, G., Checler, F. and Vincent, B. (2011) ERK1-independent α-secretase cut of β-amyloid precursor protein via M1 muscarinic receptors and PKCα/ε. Mol. Cell Neurosci. **47**, 223–232

54 Cisse, M., Duplan, E., Guillot-Sestier, M. V., Rumigny, J., Bauer, C., Pages, G., Orzechowski, H. D., Slack, B. E., Checler, F. and Vincent, B. (2011) The extracellular regulated kinase-1 (ERK1) controls regulated α-secretase-mediated processing, promoter transactivation, and mRNA levels of the cellular prion protein. J. Biol. Chem. **286**, 29192–29206

55 Glaros, E. N., Kim, W. S., Rye, K. A., Shayman, J. A. and Garner, B. (2008) Reduction of plasma glycosphingolipid levels has no impact on atherosclerosis in apolipoprotein E-null mice. J. Lipid Res. **49**, 1677–1681

56 Lukina, E., Watman, N., Arreguin, E. A., Banikazemi, M., Dragosky, M., Iastrebner, M., Rosenbaum, H., Phillips, M., Pastores, G. M., Rosenthal, D. I. et al. (2010) A phase 2 study of eliglustat tartrate (Genz-112638), an oral substrate reduction therapy for Gaucher disease type 1. Blood **116**, 893–899

57 Lukina, E., Watman, N., Arreguin, E. A., Dragosky, M., Iastrebner, M., Rosenbaum, H., Phillips, M., Pastores, G. M., Kamath, R. S. and Rosenthal, D. I. (2010) Improvement in hematological, visceral, and skeletal manifestations of Gaucher disease type 1 with oral eliglustat tartrate (Genz-112638) treatment: 2-year results of a phase 2 study. Blood **116**, 4095–4098

58 McEachern, K. A., Fung, J., Komarnitsky, S., Siegel, C. S., Chuang, W. L., Hutto, E., Shayman, J. A., Grabowski, G. A., Aerts, J. M., Cheng, S. H. et al. (2007) A specific and potent inhibitor of glucosylceramide synthase for substrate inhibition therapy of Gaucher disease. Mol. Genet. Metab. **91**, 259–267

59 Peterschmitt, M. J., Burke, A., Blankstein, L., Smith, S. E., Puga, A. C., Kramer, W. G., Harris, J. A., Mathews, D. and Bonate, P. L. (2011) Safety, tolerability, and pharmacokinetics of eliglustat tartrate (Genz-112638) after single doses, multiple doses, and food in healthy volunteers. J. Clin. Pharmacol. **51**, 695–705

Received 13 May 2011/28 October 2011; accepted 21 November 2011
Published as Immediate Publication 21 November 2011, doi:10.1042/CS20110257

online data

Clinical Science (2012) **122**, 409–419 (Printed in Great Britain) doi:10.1042/CS20110257

SUPPLEMENTARY ONLINE DATA

Dissociation of ERK signalling inhibition from the anti-amyloidogenic action of synthetic ceramide analogues

Hongyun LI*†, Genevieve EVIN‡§, Andrew F. HILL§‖, Ya Hui HUNG§¶, Ashley I. BUSH§ and Brett GARNER*†

*Illawarra Health and Medical Research Institute, University of Wollongong, Wollongong, NSW 2522, Australia, †School of Biological Sciences, University of Wollongong, Wollongong, NSW 2522, Australia, ‡Department of Pathology, University of Melbourne, Melbourne, VIC 3010, Australia, §Mental Health Research Institute, University of Melbourne, Melbourne, VIC 3010, Australia, ‖Department of Biochemistry and Molecular Biology, Bio21 Institute, University of Melbourne, Melbourne, VIC 3010, Australia, and ¶Centre for Neuroscience, University of Melbourne, Melbourne, VIC 3010, Australia

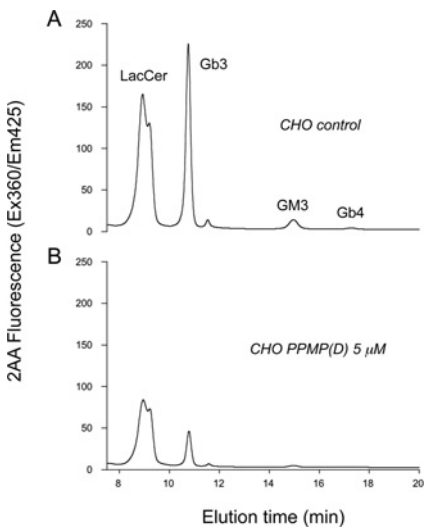

Figure S1 Inhibition of CHO-APP GSL levels by D-PDMP

CHO-APP cells were incubated for 48 h in the absence (upper profile, 'CHO control') or presence (lower profile, 'CHO PPMP(D) 5 μM') of 5 μM D-PPMP. Lipids were extracted and GSL glycans were analysed by HPLC as described in the legend to Figure 8. Gb3, globotriaosylceramide; Gb4, globotetraosylceramide; GM3, ganglioside G_{M3}.

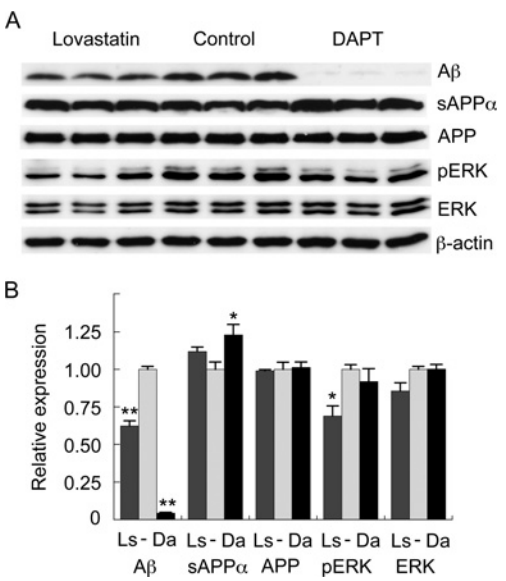

Figure S2 Influence of lovastatin and DAPT (two antiamyloidogenic non-GSL-modifying compounds) on ERK activation

CHO-APP cells were treated with lovastatin (1 μM) or DAPT (1 μM) for 48 h, and secreted Aβ and sAPPα and cellular APP and total ERK and pERK (A) were measured by Western blotting with β-actin used as a loading control. Absorbance measurements of the Western blots are shown in the histograms (B): grey bars, control; dark grey bars, lovastatin treated; and black bars, DAPT treated. Results are mean $\pm$ S.E.M. values; $^{*}P < 0.05$, $^{**}P < 0.01$.

Received 13 May 2011/28 October 2011; accepted 21 November 2011
Published as Immediate Publication 21 November 2011, doi:10.1042/CS20110257

Correspondence: Professor Brett Garner (email: brettg@uow.edu.au).